POLITECNICO DI TORINO
Repository ISTITUZIONALE

Optimal strengthening by steel truss arches in prestressed girder bridges

(Article begins on next page)

25 April 2024

Optimal strengthening by steel truss arches in prestressed girder bridges

R. Cucuzza[†], C. Costi[†], M. M. Rosso[†*], M. Domaneschi[†],
G. C. Marano[†] and D. Masera[§]

[†]Politecnico di Torino - DISEG, Turin, Italy
[§]Masera Engineering Group Srl, Turin, Italy

[*]Corresponding author: marco.rosso@polito.it

Abstract

This work focuses on the proposal and the evaluation of a new consolidation system for prestressed reinforced concrete (PRC) beams of girder bridges. The system consists of two arch-shaped steel trusses placed alongside the lateral faces of the beam to be consolidated. The arches develop longitudinally along the entire span of the beam and in elevation using the available height of the PRC cross section. The consolidation system is characterized by its own external constraints, independent from those serving the pre-existing element. The efficiency of the system with respect to parameters variability is described also focusing on the ratio between the load discharged by the consolidation system and the total applied load. Referring to a case study, the consolidation of a PRC beam is presented adopting the proposed system with respect to the usually adopted external prestressing technique. The cross sections properties of the steel arch shaped trusses are defined by means of a structural optimization process using a genetic algorithm, identifying the minimum steel consumption. Finally, a preliminary cost-benefit analysis is performed for the proposed solution for a comparison with other commonly adopted techniques.

Keywords: Artificial intelligence ● Beams & girders ● Bridges ● Buildings, Structures & design

1   Introduction

Bridges can be considered the most important components of any road infrastructure. A state of complete or partial functionality loss of such structures generates significant issues on the whole transportation network (Kashani et al. 2019). In this light, careful monitoring is of paramount importance with ordinary and extraordinary maintenance interventions in order to ensure an adequate level of functionality and safety over time. In Europe, as in the whole Western world, a considerable number of bridge structures were built between the '50s and '70s during the period of maximum development of road networks using the technology of pre-stressed reinforced concrete (Di Ludovico et al. 2010). This technique, which has been established since the '50s, was relatively young, with the consequence that the technologies, materials, and construction process could not rely on consolidated experience. In addition, the structural design process was still mainly focused on the concept of strength, giving little importance to the durability requirement (Petrangeli et al. 2019) (Petrangeli 2017). As a result, today, some decades after their construction and often at the end of their service life, many of these bridges show significant evidence of degradation with serious consequences on the safety levels and functionality. Direct evidence of such effects is provided by the different collapses that occurred in recent years in Italy, e.g. the collapse of the Fossano Viaduct in 2017 (Clemente 2020), the Polcevera Viaduct in 2018 (Domaneschi et al. 2020) and the Albiano Magra Bridge in 2020 (Gaßner & Kollegger 2021). Among the main reasons that can be identified, the loss of prestressing due to cable corrosion plays the major role (Bazzucchi et al. 2018) (Domaneschi et al. 2020) (Morgese et al. 2020). In post-tensioned structures, one of

the reasons that can facilitate this process is represented by the inadequacy of the ducts injection process during construction. Following several post-tensioned bridge collapses, the UK went so far as to prohibit the use of this technique between the years 1992 and 1996 (Petrangeli et al. 2019). At the same time, traffic volumes and the number of heavy vehicles passing through reached levels that were not foreseen in the reference standards at the time of design, further contributing to the structural deterioration (Morgese et al. 2020). A solution could be the complete replacement of the structure, but often it turns out to be the most expensive and impactful choice, not only for direct construction costs but also indirect ones such as traffic interruption, overloading of the alternative road system, etc. (Park et al. 2005). The alternative choice consists, when possible, of reinforcement interventions that can extend the service life, restoring adequate levels of functionality and safety. The definition of the reinforcement system depends on the evaluations of the designer that is related to own experience and knowledge, identifying the critical conditions, and selecting the most effective solution from the technical, constructional and economic aspects. Each consolidation intervention has advantages and disadvantages: a relatively simple intervention from the point of view of implementation (commonly used materials, common labor, easy installation, etc.) may not be sufficiently efficient in restoring the required performance levels. On the contrary, an extremely efficient intervention from the structural point of view, but which foresees the use of advanced technologies (innovative solutions, highly specialized manpower and companies for the installation, etc.), could raise the costs and make the intervention uneconomic. Based on all of the above considerations, the introduction of new consolidation techniques for existing bridge structures is a topic of crucial interest.

The present work introduces an innovative solution for the reinforcement of a prestressed concrete (PRC) beam, which often constitutes a component of most existing bridge decks. With the proposed method the uncertainty related to the damage state of bridges and, consequently, the consolidation interventions were overcome. The new strengthening system leads to restore the safety level of the structure without any knowledge about the loss of prestressing due to cable corrosion. Moreover, the proposed retrofitting system represents a competitive alternative in terms of installation complexity and even from an economical point of view. The objective is to propose a solution suitable for bridges with grid decks, i.e. composed of several longitudinal girder beams placed side by side and connected by stringers. The proposed solution consists of using two arch-shaped trusses coupled and connected to the existing beam to be consolidated, creating a parallel strengthening system to support part of the loads to which the existing deck is subjected. This kind of solution is analysed on PRC girder bridge which is the most widespread typology of existing heritage in Italy, but this strengthening system may virtually be applied even on composite girder bridges or concrete box girder bridges. Therefore, future works will address the applicability of the proposed retrofitting system to the above-mentioned bridge typologies and the relative case studies. The remaining parts of this paper are organized as follows: Section 2 deals with existing and the proposed consolidation solutions, Section 3 presents the case study with the performed finite element analysis, a parametric sensitivity analysis is the developed (Section 4) with an optimization procedure (Section 5) for the proposed consolidation technique. The remaining sections of the paper (Sections 6 and 7) are devoted to the presentation of the results with a preliminary cost comparison between the proposed solution and the traditional approach.

2 Prestressed bridge decks and consolidation solutions

Currently, most of the bridges that are built all over the world adopt pre-stressed reinforced concrete. The complete exploitation of concrete sections and of harmonic steel characteristics, the extensive use of prefabrication, the adoption of automated launching systems have made them very competitive for medium and large spans (Arici & Granata 2019). While very large spans are covered by cable-stayed and suspension solutions, smaller spans are overcome with truss, frame or arch solutions. In truss bridges, the main elements are beams, i.e. elements stressed mainly by bending and shear. The most commonly used solutions include grid or box girder decks. Focusing on the use of pre-stressed reinforced concrete as the constituent material of the beams or segments, the covered spans range from 30 to 50 m for the first type and up to about 150 m for the second. Grid decks are realized with side-by-side longitudinal beams connected by transversal elements and

the slab, this latter usually cast on-site. The longitudinal beams are generally prefabricated with I or V sections (box girder) pre-tensioned during the production process, post-tensioned on-site or adopting a mixed solution. The most frequent static scheme is the simply supported solution due to the rapidity of assembly. For this reason, such deck type was widely used in the post-second-world-war reconstruction period with the development of highway networks, from the '60s onwards. Due to their age, design and construction faults (inaccurate injection of sheaths, lack of or deterioration in the waterproofing of the deck), and poor maintenance, such bridge types have been increasingly found in critical situations (Bazzucchi et al. 2018) (Domaneschi et al. 2020) (Morgese et al. 2020). Their origins can be divided into three categories: design defects, construction defects, maintenance deficiencies (Godart 2015), while reinforcement corrosion is one of the central problems for prestressed concrete structures (Recupero et al. 2018).

Given the age of many of the existing bridges, deterioration is certainly one of the factors for which reinforcement interventions are required. Corrosion of the reinforcements or of the prestressing systems, and deterioration of the concrete due to chemical attack, lead to a progressive reduction of the load-bearing capacity and therefore of the safety margins, which must be restored in some way. However, deterioration is not the only factor that makes reinforcement interventions of paramount importance. An increase in the traffic volume and of the axle loads, prestressed losses due to slow phenomena (concrete shrinkage and viscosity), design or executive errors require the infrastructure manager to adopt traffic restrictions or implement reinforcement interventions (Daly & Witarnawan 1997).

The selection of the suitable reinforcement system needs to consider several factors (e.g. type of structure, capacity increase needed, cost of the intervention). The economic evaluation must also take into account future maintenance costs of the reinforced structure. It is important to evaluate the condition of the elements to be reinforced and other structural components, including the substructure (foundations, piers, abutments, etc.) (Daly & Witarnawan 1997) (Highways agency 1999). The inspection, knowledge and diagnosis phase of the structural condition and its components is fundamental. The reasons and origins that generated the functionality losses and safety levels reduction have to be identified (e.g. corrosion of reinforcement). Moreover, such performance reductions have to be quantified (e.g. decrease in load-bearing capacity) (Highways agency 1999). Considerations of the interventions in terms of interference with traffic flow and also aesthetic evaluations are relevant in the choice of the appropriate technology.

The following subsection presents a consolidation method widely used to remedy performance losses of existing bridges with prestressed grid decks, mainly related to corrosion degradation. Subsequently, the proposed solution, which is the subject of this paper, will be introduced.

2.1 Traditional consolidation systems for bridge decks: external prestressing cables

Adopting the external prestressing solution, the cables are external to the section and not adherent to the concrete bulk. As for traditional prestressing solutions, also in this case an axial load is applied in order to obtain a favorable pre-load, increasing the flexural capacity and improving the performance under service loads (Daly & Witarnawan 1997). In general, the external prestressing solution can be considered as the coupling of two subsystems: the concrete beam and the external cables (Pisani 1999). The prestressing force is not transmitted by adhesion but through a system of anchors and deflectors. Therefore, the profile of the external cables consists of straight paths.

The external cables transmit to the concrete beam, at the anchorages and the deviation points (deviators), concentrated forces whose intensity depends on the tensile forces in the cables and the shape of their path.

One of the main disadvantages has been identified in the increase of tensile forces in the reinforcement as the load increase depends on the overall elongation of the cable, which in turn is a function of the deformability of the entire structure and not just the section under consideration. The tensile increase is considerably lower than that which would occur in a structure with adherent cables and the calculation is not immediate. A further disadvantage is given by the reduction of the eccentricity of the cable as a result of deformation of the structure, especially if there are few points of deflection (Alqam & Alkhairi 2019).
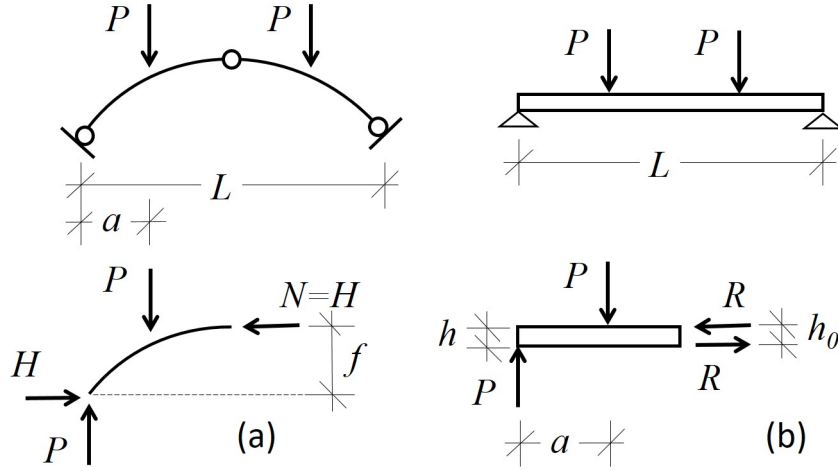
Figure 1: Comparison between a three hinged arch beam and (a) a simply supported beam (b) under a symmetric load configuration.

The addition of external prestressing as a technique for reinforcing existing bridges has seen significant adoption in recent years owing to several advantages (Daly & Witarnawan 1997) (Khudeira 2010). For example: (i) there is an increase in flexural capacity without significant increases in self-weight; (ii) the components are easy to inspect and any damage is easily detected; (iii) the process of installing the reinforcement system can be conducted without interrupting traffic; (iv) the in-service behaviour can be corrected. However, the installation of the reinforcement system must be performed by expert labor in using this technique. Furthermore, the concrete material must be in good conditions to withstand the stresses deriving from additional prestressing.

2.2   Proposed consolidation system for bridge decks: steel arch trusses

In this work, a new consolidation system for bridge decks is proposed, which consists of two arch-shaped steel trusses linked to the beam to be consolidated. A FEM analysis was conducted in order to evaluate the load distribution between the arches and the beam and calculate the beneficial effects of the strengthening with suitable performance ratios. Although the external prestressing cables technique aims to restore the capacity and the structural efficiency of the damaged beam, the proposed consolidation technique is intended to reduce the external load carried by the existing PRC beam. The static behaviour of the arch offers several advantages respect to the straight barycentric axis beam one (Cucuzza et al. 2021). Referring to Figure 1, by comparing the static behaviour of a three hinged arch with the a straight beam with the same span, geometrical section and load pattern one obtains:

$$\sigma_a = \frac{Pa}{Af}; \qquad \sigma_b = 6\left(\frac{Pa}{bh^2}\right)$$
$$\sigma_b = \sigma_a \left(\frac{6f}{h}\right). \tag{1}$$

where σ_a and σ_b indicate the stress at the midspan of the arch and the beam respectively. Hence, being that $f >> h$, the straight beam results significantly more stressed with respect the three hinged arch due to the fact, as depicted in Figure 1, for the first case, the external moment Pa is balanced by the internal moment Rf, while, in the second case, a higher balanced moment is guaranteed by Hf. For example, in the case of two hinged arch, the thrust H at external restraints generates internal actions of bending moment and shear that are opposite to the same load-induced by the external force. In the case study of interest, the effective stresses acting at the level of the
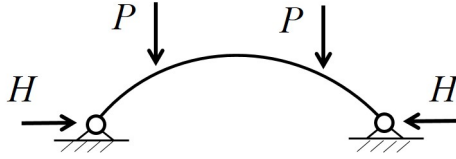
Figure 2: Static scheme of a two hinged arch under symmetrical load configuration. The constraints avoid horizontal displacement at the level of the fixed hinges.

arch have been calculated as follow:

$$M = M_0 - Hy; \qquad V = V_0 - H\sin\theta;$$
$$N = N_0 - H\cos\theta \tag{2}$$

where y indicates the vertical distance between the fiber of the investigated section and the fixed hinges; θ is the angle between the tangent at the barycentric fiber of the considered arch section and the horizontal axis; M_0, V_0, N_0 indicate the bending moment, shear and tension stress respectively due to vertical external load or vertical reaction without taking into account any horizontal component (H).

Moreover, several advantages in terms of deformability are offered by an arch beam with respect to the straight beam simply supported. Comparing the vertical displacement due to a concentrated vertical force applied at the middle span of the straight beam (δ_t) with the, previously cited, parabolic arch static scheme (δ_a) neglecting shear and axial deformability, one obtains:

$$\delta_b = \frac{Fl^3}{48E_bI_b}; \tag{3}$$

$$\delta_a = \frac{Fl^3}{2048E_aI_a} \tag{4}$$

where l indicates the beam span, E_b and E_a represents the elastic modulus of the beam and arch materials respectively, I_b and I_a are the beam and arch moments of inertia respectively.

Combining Equation 3 and 4 the following relation can be found:

$$\delta_a = \frac{3}{128}\delta_b \tag{5}$$

which demonstrates the higher stiffness of the arch solution despite to the straight beam one. Although the main differences in terms of structural behaviour between arches and straight beams are evident, the interaction between these two different structural elements and how they work together has not yet been fully investigated. With a preliminary study, the interaction between two hinged arches placed alongside the main simply supported beam, having the same span and under a symmetrical load condition, is herein investigated. The PRC beam and the lateral arches are bound together along their longitudinal length as a consequence that they are constrained to work together and thus sharing the external load according to their stiffness. The load distribution is carried by a structural system composed by two sub-systems that work in parallel. Therefore, the splitting percentage of the force F is a function of the stiffness elements and/or their different displacements. Simplifying the Equations 3 and 4, one obtains:

$$\delta_a = \frac{F_a}{K_a}; \tag{6}$$

$$\delta_b = \frac{F_b}{K_b} \tag{7}$$

where K_a and K_b represent respectively the arch and beam's stiffness while F_a and F_b indicate the percentage of the force F carried respectively by the arches and the beam. Due to the hypothesis of rigid connection, guaranteed by an anchoring system of the arch to the PRC beam, the following conditions must be satisfied:

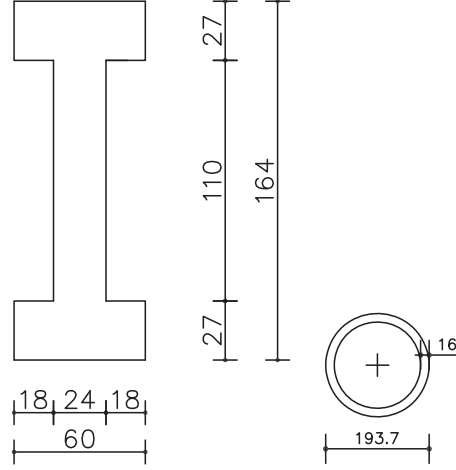$$\delta_a = \delta_b = \delta \tag{8}$$

5

Figure 3: Double-T-shaped section of the concrete beam (on the left). Dimensions are expressed in [cm]. Circular hollow section (CHS) of the steel arch beam (on the right). Dimensions are expressed in [mm].

Double T section	
E_t[Mpa]	$3,2836 * 10^4$
I_t [mm^4]	$1,806 * 10^11$
K_t [N/mm]	$6,102 * 10^3$

Table 1: Geometrical features of the concrete beam.

Moreover, in order to respect the vertical translational equilibrium, the load distribution between arches and beam is defined as following:

$$F = F_b + 2F_a = (K_b + 2K_a)\delta = K\delta \tag{9}$$

where K represents the equivalent stiffness of the beam-arches assemblage and δ the global displacement system. In this way, it is possible calculate the load distribution between arches and beam as a function of their independent stiffness and also determine the equivalent one of the whole structural system.

$$F_a = K_a\delta = K_a \frac{F}{(K_t + 2K_A)}; \tag{10}$$

$$F_b = K_b\delta = K_b \frac{F}{(K_b + 2K_A)} \tag{11}$$

In order to achieve a major awareness about the efficiency of the proposed strengthening system, a numerical example has been conducted considering a simply supported beam of 36 m span consolidated with two double-hinged arches placed one on the left and on the right the main beam. The material and the geometrical features of the main beam and arches respectively are reported in Tables 1, 2 and depicted in Figure 3. With the aim to evaluate the distribution load between

Tubolar section 193x16 mm	
E_a[Mpa]	$2,100 * 10^5$
I_a [mm^4]	$3,554 * 10^7$
K_a [N/mm]	$3,276 * 10^2$

Table 2: Geometrical features of the steel arches.

arches and beam, in Table 3, the ratios K_a/K and K_b/K have been calculated considering the connection system previously described.

It is worth noting that, nevertheless the arch and beam's stiffness showed a gap of about one order of magnitude, the arches are able to carry a reasonable percentage of the external load F

6

Load distribution of F	
$2K_a/K$	$0,10$
K_t/K	$0,90$

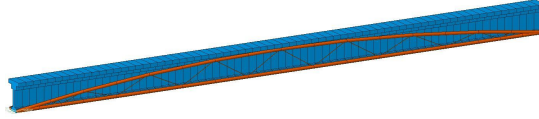Table 3: Distribution load between beam and arches.

Figure 4: Prospective view of the main beam with the strengthening system proposed

(evaluated almost the 10 % of the total force). In other words, the consolidated concrete beam has been relieved approximately of the 10 % with respect to the unconsolidated configuration.

Finally, the numerical example shows how, in order to retrofit a simply supported beam, the stiffness of the consolidation system plays a fundamental role in achieving the best structural performance and/or efficiency. Therefore, the strengthening system proposed in this work should perform according both to functionality and rigidity. This system results quite suitable to girder bridges composed of several spans sustained by different prestressed concrete beams with a maximum length of approximately $35 - 40$ m. The static scheme appears mostly as a simply supported beam for each span with variable height values between $1, 2 - 2, 5$ m. For these reasons the arches have the same height as the main beam and are stiffened by inclined trusses in order to reduce the deformability of the whole beam-arches assemblage as depicted in Figure 4. The consolidation system is suitably linked to both sides of the main beam with rigid anchoring beams with the aim to guarantee the transfer of stresses from the main element (PRC beam) to the secondary ones (trussed arches). Both beam and arches result equipped with different bearing devices placed at the top of the pillars (or abutments).

Although the two hinged arches provide the most stiffened static scheme, remarkable horizontal forces due to the thrust of the arch are absorbed by the restraints. To avoid this critical phenomenon, a tension tie lower chord was placed achieving a static scheme with arched thrust eliminated. In this way, a very stiffened tension chord tie rod provides a structural solution that performs similarly to the two-hinged arch beam instead of the more deformable solution with a lower structural efficiency.

3 Case study and modelling using MIDAS and OpenSees

In this section, the case study and FEM modelling are described. With the goal of providing a realistic scenario, a beam belonging to an existing girder bridge located in Piedmont in Turin province (Italy) has been investigated. The deck consists of 4 statically determined simply supported spans with variable lengths of 38 m, two consecutive spans of 31 m and the final one of 30 m respectively. Each beam is a post-tensioned PRC beam connected each other by transversal beams located at three points: two at the extremity of the main beam in correspondence of pillars or abutments and one intermediate at midspan of the main beam. Due to the critical length of the first span, this latter has been selected to focus the analysis. The deck consists of 8 longitudinal beams with a double-T-shaped section whereas the transversal ones exhibit a rectangular section. In particular, considering an hypothetical transversal section of the deck, in order to check the performances of the proposed strengthening system, the external main beam of first chosen span is considered in the current work. Several technical drawings related to the selected concrete beam, reinforcement and prestressing internal reinforcement tendons have been consulted achieving a suited knowledge level of the existing structure. The main geometrical and material features of each structural element are reported in Figures 5, 6 and in Tables 4, 5.
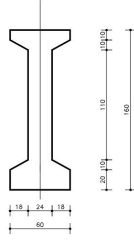
Figure 5: Double T section of the investigated concrete beam.

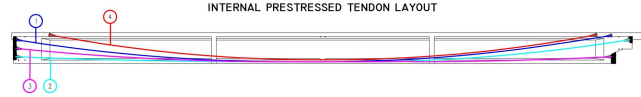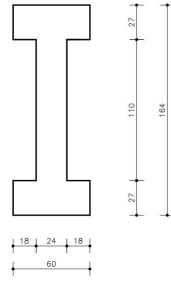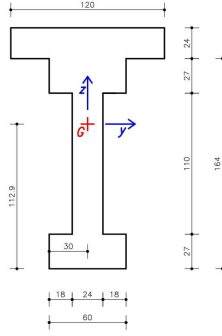Figure 6: Longitudinal section of the investigated concrete beam and tendon profile.

Figure 7: (a) Geometrical section 5 after semplifications, (b) Geometrical section modeled taking into account the effective width of the concrete slab.

Concrete C30/37 and steel S355			
f_{ck} [Mpa]	f_{yk} [Mpa]	E_{cm} [Gpa]	E_s [Gpa]
30, 0	355	32, 8	210

Table 4: Concrete material characteristics of the main beam.

Strand Y1860S7				
d [mm]	A [mm^2]	f_{pk} [Mpa]	$f_{p0,1k}$ [Mpa]	E_{cm} [Gpa]
15, 2	139	1860	1640	196

Table 5: Steel material characteristics of strands.

3.1   Not consolidated beam model

FEM structural analyses, according to Italian Code and Eurocodes, have been conducted with the MidasGen$^©$ software, a "general purpose" numerical code. At first, a tapered beam was modeled adopting a simplified section as depicted in Figure 7. Later, tendon property and profile were assigned to the tapered beam with respect to the real coordinates provided by the technical drawings. All the geometrical and material features related to the concrete beam and prestressing cables, described previously, have been assigned to the element. All the long-short term prestressing losses were considered in the modelling. Each cable lied on the same vertical plane without any type of transversal offset.

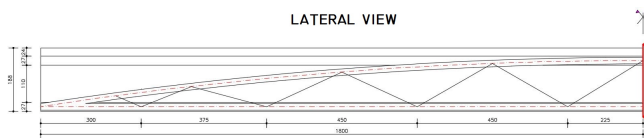The load pattern considered is composed by self-weight (SW) and uniformly distributed load Q

Figure 8: Longitudinal view of half strenthening system with the concrete beam in the background
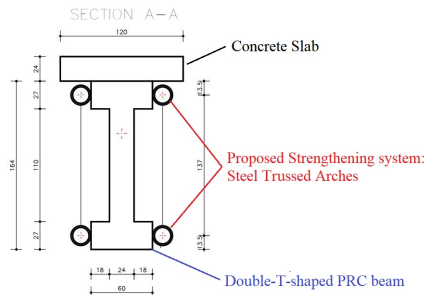

Figure 9: Transversal section at midspan of both PRC beam and strengthening system. Dimensions are expressed in [cm].
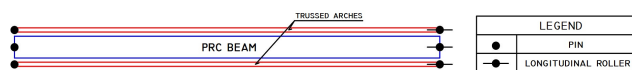

Figure 10: Plan view scheme of the external boundary assigned to each structural element.

equal to $10kN/m$ simulating live loads. In this preliminary phase, the value of live loads was chosen in an arbitrary manner in order to perform the efficiency of the proposed system. The effects of the internal forces due to the prestressing system were added to the external load configuration.

3.2 Strengthened system by steel trussed arches model

The proposed consolidation system consists of a steel structure with an arched with thrust eliminated static scheme. The compression and tension chords were stiffened by steel trusses as in the Nielsen truss structure (Franciosi 1971). As described before, steel arches and the concrete beam work in parallel, hence the maximum height at the midspan coincides with the total height of the main beam without taking into account the thickness of the deck. Moreover, as the compression chord exhibits a parabolic shape profile with the arch axis, depicted with the red dashed line in Figure 8, it passes the midspan at the intermediate point of the upper flange thickness whereas the tension chord develops along the intermediate point of the lower flange thickness. The lower tie chord presents the same length span of the beam to be consolidated. The deck represents a natural obstacle that limits the height of the crown. As shown in Figure 9, it appears clear how the slenderness of the arch strongly depends on the deck thickness: the ratio f/l, between the raise and the length span of the arch, plays a fundamental role in increasing the percentage of external load carried by the consolidation system. Higher slenderness ratio values allow taking advantage of benefits due to the arch shape behaviour. As a result that only vertical concentrated or distributed load are taken into account in the modelling, both main beam and arches were constrained with external boundary realized with fixed and sliding longitudinal supports (Figure 10). Due to the absence of transversal loads (as wind or earthquake) any boundaries that limit transversal displacements were modeled. Although the final properties of the proposed strengthening system are discussed in the next sections as a result of an Optimization process in order to maximize the efficiency of the system, in this preliminary design phase, a first attempt was conducted choosing several suited industrial solutions that respect the geometrical limits imposed by the problem. In Table 6, the material and geometrical features of the steel arches have been summarized.

With the aim to take into account the real behaviour of the compression and tension chords a *general beam/tapered beam* FEM element is used. *Truss* elements were used in order to carry

9

Figure 11: Longitudinal view of the Strengthening system MidasGen$^{©}$ model.

Tubolar section type 193x16 mm	
A [mm^2]	I [mm^4]
$8,932x10^4$	$3,554x10^7$
Truss section type ϕ 22	
A [mm^2]	
$3,801*10^2$	

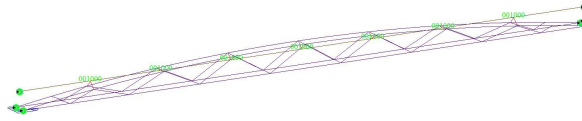Table 6: Geometrical properties steel arch and truss section type.

Figure 12: Prospectical view of the Global MidasGen$^{©}$ model. In the Figure, the fixed and sliding boundaries are depicted with green-filled circles; red lines are used to indicate the *rigid links* as connections between beam and arches.

normal stress and improve the flexural stiffness of the whole structure. Reducing the deformability of the whole system allows increasing the efficiency of the strengthening system due to a significant decrease of the concrete beam stress level.

3.3 Concrete beam connected to the strengthening system

After defining the modelling and assigned the preliminary properties to the model, the first analyses are performed. As described before, the PRC beam and steel arches work in parallel: the purpose of the consolidation system is to cooperate with the concrete beam when it is subjected to damaging phenomena or when unexpected live loads acting on the bridge. In order to achieve this goal, *rigid link* were provided allowing the load transfer thanks to the relative vertical displacement constraints between concrete beam and arches. In practice, these constraints could consist of transversal beam with the purpose to connect the two lower flanges of the double-T-shaped section with the arches. When a beam capacity reduction occurs due to a possible damage, the beam will exhibit an increasing vertical displacement that could be virtually limited by the connection of these supporting elements to the strengthening arches. Moreover, the stress transfer process between the main beam and the strengthening arches is further improved by including some other connections also at the level of the PRC beam web as depicted in Figure 12 where only the barycentric axis of each element are shown. The modelling and the position of these internal constraints have been investigated in the present work. It is worth noting that, in a detailed design phase, a specific description and calculation of these connections is requested: the stress configuration under traffic loads, effects related to the load repartition and distribution among the different structural elements certainly could provide concentrations of actions and/or local instability issues. In this investigation phase, the focus of the study was mainly conducted on the global behavior of the PRC beam-arches without a detail model of the connections.

The application of a preliminary external load as uniform live load equal , with intensity equivalent to $10kN/m$, must be considered acting to the beam after the installation of the strengthening system. In this preliminary study, the effect of prestressing and self-weight has been neglected in order to evaluate the beneficial effect of the consolidation system under vertical load only, e.g. traffic loads, snow load, etc. Subsequently to the loading Assignment phase, stress and deformability effects induced by the variable loads are evaluated. As it could be expected, the beneficial effects of the strengthening system are verified (in particular, a decrease in the vertical displacement and bending moment at the midspan have been highlighted). In this way, the arches captured a quite significant percentage of the applied variable load. As shown in Table 7, a comparison between the
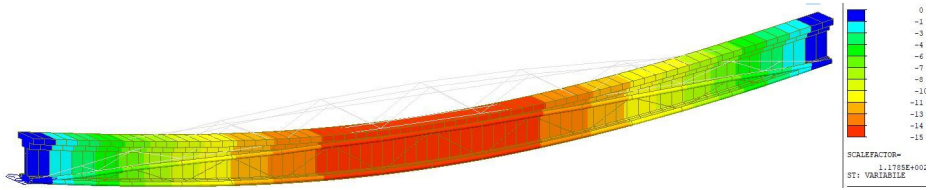
10

Figure 13: MidasGen$^©$ plot of the vertical displacement of the Retrofitted beam under a preliminary uniform live load of 10 kN/m. Values are reported in [mm].

Comparison between Not consolidated and retrofitted beam configuration

	Not consolidated beam	Retroffitted beam
$\delta_{(z,var)}(l/2)$ [mm]	-18	-15
$M_{(y,var)}(l/2)$ [kNm]	+1620	+1356
$R_{(z,1\ var)}$ [kN]	+180	+163
$R_{(z,2\ var)}$ [kN]	+180	+163

Table 7: Comparison between the unconsolidated and Retrofitted beam configurations.

two investigated configurations is conducted and the magnitude of the reduction of the vertical displacement and the bending moment in the critical section (midspan) is about 16% .

As shown in Figure 13, and summarized in Table 7, after the installation of the strengthening system, a partial reduction in terms of displacements and stresses of the main beam is recognised. Specifically, the compression and tension chords exhibit low symmetric values of bending moment despite the slenderness value imposed is not the optimal one whereas, on the contrary, important normal stresses are generated. Moreover, truss elements provided a more stiff behaviour to the whole system, respecting the theoretical previsions. It is worth noting that the performance ratio of each structural element resulted unsatisfactory due to the fact that the industrial solution implemented is not the optimal one. For this reason, A further optimization process will be necessary.

This preliminary results have shown that the idea of coupling the arch shape to the damaged beam could provide interesting developments. Unfortunately, the simplified hypothesis of external load acting simultaneously after the installation of the strengthening system does not comply with the real construction stage of the structure. The aim of the present work consists to propose a new type of consolidation technique as an alternative of the traditional external prestressing one. Therefore, the actual installation of a retrofitting system occurs only after an important loss of the capacity and/or serviceability. For this reason, a new construction stage is realized with the purpose to evaluate the efficiency of the strengthening system for an increasing value of the external loads by simulating a damage state that evolves over time.

In the software MidasGen$^©$ the *construction stage* procedure allows to define several *Elements, boundary and load groups* with the aim to take into account a certain effect due to a static scheme change, to the activation of additional load configuration or boundaries which act at a certain time or to material properties that are strongly time-dependent such as the prestressing cables. Generally, taking into consideration all these effects, it enables to consider and investigate the real stresses evolution which occurs in the structure during the damage evolution and after the strengthening system installation. For this reason, two main construction phase were defined:

Construction stage 1: at this phase, the main concrete beam was modeled without any strengthening system. Specifically all the external boundaries and load pattern, which consists into self-weight and prestressing cables, were activated at the same time as the starter point for further investigations.

Construction stage 2a: at this phase, the installation of the strengthening system was modeled. Both arches are supported by fixed and sliding supports, independent to the concrete beam external boundaries, which were assigned at the previous phase. During the installation stage, the concrete beam is loaded with the same load pattern already previously defined. On the contrary, arches were subjected to self-weight and still does not present any type of connection with the main structural beam element. At this stage the arches and the PRC beam are still non-connected and, therefore, act independently.

Comparison between Not consolidated and retrofitted beam configuration

	Not consolidated beam	Retroffitted beam
$F_{Z,1,SW+Prest}$ [kN]	+394, 2	+369, 9(−6%)
$F_{Z,2,SW+Prest}$ [kN]	+394, 2	+374, 0(−5%)
$M_{y,SW+Prest}(l/2)$ [kNm]	+78, 0	−263, 0

Table 8: Deactivating effect of cables 1 and 4 (−43%)

Construction stage 2b: the connection between the main PRC beam and the strengthening system was modeled. In this construction stage, *rigid links* were activated when the main structural element achieved a first stress and strain state. From this moment forwards, any load distribution changes is recognised: each load increment detected or any activation of new different load patterns will allow to evaluate the beneficial effect of the strengthening system. It is worth noting that, compared with the previous models in which concrete beam and arches were modeled simultaneously but act separately, in this phase the consolidation system acts when the main beam exhibit a certain stress and strain state and any future damage effect, e.g. the cables relaxing, will be detected.

Construction stage 2c: in this final step, the cooperation between the consolidation system and the main beam is investigated. Applying an uniform distributed load, the beneficial effect of the retrofitting system can be investigated. Moreover, potential prestressing losses, resulting in an unbounded configuration of one or more cables, can be studied by deactivating the cables and providing a comparison between the different previous configurations. In this way, deactivating some strands of a certain cable means that it will result in an unbounded situation for the the whole considered tendon profile.

A prestressing loss of cables 1 and 4, as reported in Figure 6, equivalent to the 43% of the normal stress at the midspan of the concrete beam for both the Not consolidated configuration and the retrofitted one is considered. The comparisons are summarized in Table 8 where beneficial effects of the consolidation system are described. In conclusion, the vertical reactions, obtained considering only self-weight and prestressing effect acting on the PRC beam, calculated at the edge of the main beam, receive a decrease of about the 6%, which is consistent with the conducted preliminary analysis.

4   Parametric and sensitivity analysis using OpenSees© and Matlab©

In the previous section, it was shown the beneficial effects of the proposed strengthening system without any specific considerations about the geometry, section properties and material assigned to each structural element. A *sensitivity analysis* is herein conducted with the purpose to investigate which are the variables that mainly affect the analysis. In this way, in the present section, the applicability field of the proposed system is discussed and, in particular, it is investigated what are the best industrial solution for a preliminary design. Since the proposed consolidation system appears to be suitable for girder bridges, the slenderness ratio plays a main role in the preliminary design. For this reason, a preliminary survey inherent the most usual slenderness ratios adopted for this kind of bridge was useful in order to define the lower and upper limit of this variable range. Summarly, the input variables that were taken into account in the sensitivity analysis are:

Beam length span (L): the investigation includes all the girder bridges with a value of beam span between the upper value of 42 m and the lower one of 28 m with successive increases of 1 meter step. In this way, the best representative range of Beam span was achieved. As discussed before, fixing the concrete beam span length, it consequently also set the length of the tie rod of the trussed arches.

Steel arch rise-length span ratio f/L: once defined the span length and the height of the concrete beam, automatically the arch slenderness ratio results well defined. In order to conduct the study with the most representative values, the following values for the ratios are chosen: 0, 04 ; 0, 05 ; 0, 06 ; 0, 07.
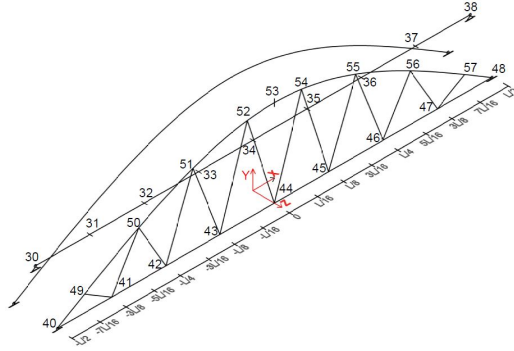
Figure 14: Parametrization of the model adopted in OpenSees$^{©}$.

Geometry and section of each element composing the strengthening system: compression and tension chord are chosen as input parameter of the problem due to the fact that, differently from trusses, they have the most influence on the global stiffness of the steel arches. Specifically, the external diameter of the tubular steel arch section varies between 150 mm up to 300 mm with successive increases of 50 mm each step.

External boundary of the trussed steel arches: Several static schemes are investigated providing also a double-pinned supports at the edges of the strengthening system simulating a two-hinged arch behaviour.

All the input parameters are summarized in Table 9:

Input parameter of the *sensitivity analysis*	
$f(h)/l$	*Area* $[mm^2]$
0, 04	$\phi150t.16 = 6732$
0, 05	$\phi200t.16 = 9249$
0, 06	$\phi250t.16 = 11762$
0, 07	$\phi300t.16 = 14275$

Table 9: Summary of input parameter of the sensitivity analysis.

4.1 Parametrization of the strengthening system

The parametrization of the geometrical model is conducted considering the span length (L) and the height (H) of the main beam as dominant parameters. When L is assigned, in fact, the coordinates of the external supports are defined, whereas setting the beam height automatically defines the position of the arch rise. Once the coordinates of these three points are identified, the parabolic profile of the steel arches can be drawn. Finally, a reference system is defined with the origin of axis placed at the intrados midspan of the main beam, with the X axis directed along the longitudinal direction of the beam whereas Y axis is vertical and perpendicular to the X direction. In Figure 14, the defined parametrization and the coordinates of each node of the structure have been illustrated.

In order to develop a suitable parametric model, it was adopted the object-oriented software framework open source *OpenSees*$^{©}$ developed by Berkeley University. The connection realized between *Matlab*$^{©}$ and this FEM numerical code was extremely useful to post-process the *.tcl* output files, which stores the linear static analysis results. Furthermore, Matlab$^{©}$ allows to automatically manage and iterate many analysis characterized by different FEM models because they are function of the variable input parameters above-mentioned. Each constant value (geometrical section, material, etc...) and parametric variable defining the geometry of the structure have been implemented into the software. The loading pattern is associated to a time series in order to solve the structure at each step of the increasing of the uniform distributed load value.

In this paragraph, the results obtained by the conducted static analysis of the parametric model are discussed. The sensitivity analysis allows to understand which are the variables that mainly

affect the solution and, in particular, which are the relationships among them. The efficiency of the system is evaluated considering a new index, which considers the percentage of the external load carried by arches. In this way, evaluating the *efficiency index* (*E.I.*) for each input parameter, it is possible to determine which variable will be dominant or negligible. This *efficiency index* is calculated as:

$$E.I. = \frac{\sum R_{y,arches}}{qL}, \tag{12}$$

where $\sum R_{y,arches}$ are the sum of the steel arches vertical reactions developed by the external supports, q is the intensity of the distributed load equivalent to 10 kN/m in these preliminary evaluations and L is the beam span length.

This performance parameter allows to evaluate two extreme scenarios: when its value is equal to zero, any external load is transferred from the main beam to the strengthening system, thus the consolidation system is completely inadequate to fulfill its role. On the contrary, when the value of the efficiency index is equal to 1 the whole external load is carried by the arches with a concrete beam that results in a zero stress and strain configuration. The trend of this performance parameter is investigated within the *sensitivity analysis*:

Dominance of the slenderness ratio f/l and the boundary condition: the trend of the efficiency index by varying length beam span and f/L are depicted in Figure 15. As said before, the slenderness ratio f/L of the arches respects the variable range of the slenderness ratio H/L of concrete beam which represents the widespread case studies in the field of the girder bridge. The diameter adopted to the compression and tension chords is 200 mm and it must be considered as a constant value for each iteration. A comparison between the static scheme including a sliding and a pinned support and the both double-pinned static scheme one is provided. As expected, results show that the double-pinned supports static scheme is the stiffest: the E.I. achieves the highest values rather than the static scheme with sliding and a pinned support. In the first configuration, the strengthening system is able to capture 32% of the entire external load acting to the concrete beam instead of only 20% detected in the second case. The E.I. shows a moderate dependence by the variable beam length and the slenderness ratio f/L. Specifically, with the increase of L, the efficiency index decreases about 6 or 4% respectively in the first and in the second investigated static scheme. Considering the reference case study of the present work, it is characterized by a ratio f/L equal to $0, 04$ and the obtained efficiency index varies between 32% at 28 m up to 29% at 42 m of the beam span length. Since the strengthened structure works as a parallel system, this moderate variability depends on the stiffness ratio between beam and arches. Setting a constant value of the slenderness ratio f/L, when concrete beam span length L increases, it provides a higher stiffness and the arches will carry a bigger percentage of the external load compared to the situation when the arches results unloaded. In Figure 15, the steel arches slenderness ratio f/L can be studied. The efficiency index shows a low decreasing trend: when the f/L ratio is higher, the height of the beam increases in a non-proportional manner. Consequently, for a little increase of the arch stiffness, a bigger increase of the moment of Inertia of the concrete beam section occurs which explains the decreasing trend of the investigated parameter. A lower fraction of the entire external load is captured by the strengthening system.

Dominance of the geometrical arch section (A): the trend of the efficiency index by varying the sectional features of the compression and tension chord of the strengthening system has been investigated. Fixing the f/L ratio equal to $0, 05$, the external diameter of the tubular section has been varied between a lower value of 150 mm to the upper one of 300 mm. Similarly to the previous case, the dependence of the solution by the restrained static scheme is analysed. As depicted in Figure 16, it is shown that with increasing value of the external diameter, the fraction of the entire external load captured by the arches increases. The increase of the external diameter brings to more stiff arches due to an increment of the Moment of Inertia which justifies higher values of the efficiency index. As in the previous case, the double-pinned supports static scheme results the stiffest solution although the thrusts at the fixed support are higher. In the case of a beam span length of 28 m and a tubular section of arches equal to 300 mm, the fraction of the external load carried by the strengthening system is equal to 37% for a double-pinned supports static scheme than the second one in which is equal to 25%.
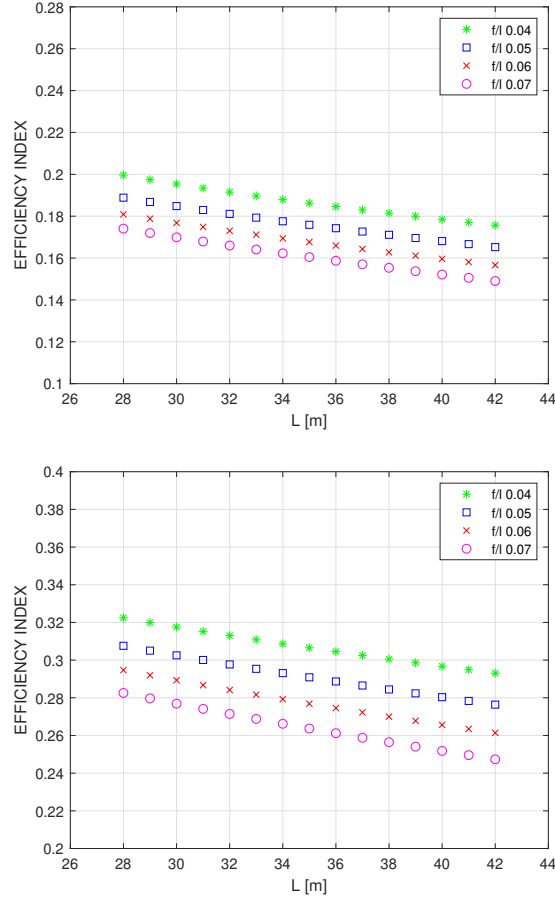
Figure 15: Trend of the efficiency index with variable slenderness ratio (f/L) and beam length (L), constant value of the compression and tension chords equal to 200 mm and external load equal to 10 kN/m in the pin-roller static scheme (on the left) and double-pinned one (on the right).

In conclusion, it is worth noting that the sectional features of the compression and tension chords represent the dominant parameters which mostly afflict the solution. A higher value of A means a higher value of the efficiency index, whereas a moderate influence on the efficiency index is performed by the slenderness ratio f/L or by external boundary. Obviously, the choice of the sectional features of each structural element composing arches must be defined as a function of the level of stresses recognised by the whole structure. In the further section, the preliminary design of the strengthening system will take into account not only the distribution load between concrete beam and arches but also the stress and strain check imposed by the Civil Codes and possible damaging conditions which affect the existing bridge heritage.

5 Degradation simulation and retrofitting with traditional intervention

Since the analyzed case study is referred to an existing structure, it is highly probable that this structure is affected to a certain ordinary level of degradation with respect to the original construction conditions. In order to take into account this fact in a simplified way, it is convenient to simulate the current damaged conditions referring to a reduction of the ultimate resisting moment M_{Rd}. Similarly to other studies about rebar losses due to corrosion, e.g. (Zhao et al. 2018), the resisting moment reduction is directly taken into account by a reduction of the actual resisting steel reinforcement area with respect to the original one. In this study, four different levels of degradation
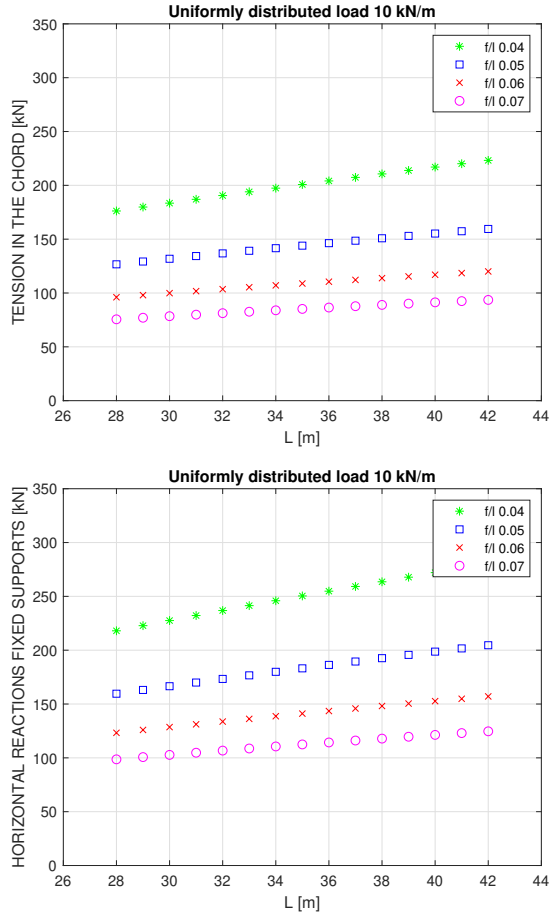
Figure 16: Trend of the efficiency index with variable geometrical area and beam length (L), constant value of the slenderness ratio (f/l) equal to 0,05 and external load equal to 10 kN/m in the pin-roller static scheme (on the left) and double-pinned one (on the right).

Simulated degradation levels	
Degradation level	Resisting steel area reduction [%]
1	5%
2	10%
3	15%
4	20%

Table 10: Four simulated degradation levels.

have been identified as reported in Table 10. Since the structural scheme is a simply supported PRC beam under a unique load condition for sake of simplicity (self weight and uniformly distributed load equal to 52 kN/m), the midspan section is the most stressed one. Therefore, the structural performance evaluation is reconducted to the analysis of the ratio M_{Sd}/M_{Rd} between the acting moment M_{Sd} and the resisting moment M_{Rd} in the midspan cross section. Due to the progressive increase of the deterioration level, when the performance ratio becomes greater than one, safety levels are no more satisfied a retrofitting intervention becomes strictly necessary in order to bring back the performance ratio below one. Referring to the original conditions (undamaged) and the simulated damaged induced situations, Table 11 illustrates the performance ratios for the unconsolidated PRC beam. As shown in the Table, the safety level is respected only for the undamaged condition and for the degradation level 1. Considering the damage level 3 as a reasonable ordinary damage level, it is possible to analyze an initial retrofitting intervention with the traditional

Performance ratio for the unconsolidated situation

Degradation level	M_{Sd} [kNm]	M_{Rd} [kNm]	$\frac{M_{Sd}}{M_{Rd}}$
Undamaged	11'995	12'621	0,95
1	11'995	12'145	0,99
2	11'995	11'632	1,03
3	11'995	11'094	1,08
4	11'995	10'541	1,14

Table 11: Performance ratio for the unconsolidated situation for different degradation levels.
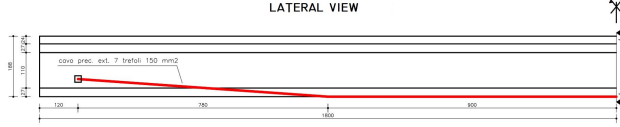

Figure 17: External prestressed cables layout profile (red solid line) adopted as a traditional intervention proposal .

Summary of the traditional intervention

P_{ext}	$2 \cdot 550 = 1100$ kN		
Anchorages		Deviators	
N_{ext}	V_{ext}	N_{ext}	V_{ext}
1097	77	3	77
Barycenter elevation [m]		Eccentricity (Midspan sec.) [m]	
$y_{G,\text{midspan}}$	$y_{G,\text{cables,anchorages}}$	e_{ext}	
1.129	0.55	1.131	
$M_{\text{ext},1}$ [kNm]	$M_{\text{ext},2}$ [kNm]	$M_{\text{ext},3}$ [kNm]	M_{ext} [kNm]
635	1299	-693	1241

Table 12: Summary of the mechanical and geometrical properties of the external prestressed cable intervention.

technique of external prestressed cables in order to bring back the performance ratio of 1.08 to the initial undamaged value (0.95). The intervention proposal is depicted in Figure 17, where the symmetrical piecewise linear tendon layout profile is composed by two external tendons with 7 strands each of 0,6 inches. The prestressing force P_{ext} of each tendon at the anchorages is 550 kN. The deviators are placed at $L/4$ from the extremity of the beam. The effects of external cables intervention has been considered with the equivalent load method, thus as further external actions of axial force N_{ext} and bending moment M_{ext}. This latter is given by three contributions: $M_{\text{ext},1}$ is related to the eccentricity of the cable ($e_{\text{ext}} = M_{\text{ext}}/N_{\text{ext}}$), $M_{\text{ext},2}$ is given by the shear force induced at the anchorages whereas $M_{\text{ext},3}$ is given by the shear force produced in correspondence of the deviators. The traditional intervention with the above-mentioned characteristics, summarized in Table 12, has been identified to be able to bring back the performance ratio to its undamaged level as shown in Table 13. Considering always the same degradation level 3, this traditional intervention is compared from a structural point of view with the strengthening method of steel trussed arches proposed in the current study. The characteristics of this latter intervention proposal is determined by an optimization procedure in order to define the most suitable solution for this kind of intervention. From the technical point of view, whereas the external prestressed cables intervention acts as external induced actions and plays a role directly on increasing the resisting moment, the proposed steel trussed arches solution generates a reduction of the acting moment M_{Sd}. Since the arches work in parallel with the PRC beam, the acting loads on the whole strengthened system undergo a repartition process governed by the relative stiffness of the arches and the beam. With respect to the unconsolidated situation, this phenomenon leads to a decrease in the beam carried load without affecting in any way the beam midspan cross section ultimate resisting moment.

Performance ratio for the post-intervention with external prestressed cables

M_{Sd} [kNm]	$M'_{Sd} = M_{Sd} - M_{\text{ext}}$ [kNm]	M_{Rd} [kNm]	$\frac{M'_{Sd}}{M_{Rd}}$
11'995	10'754	12'145	0,95

Table 13: Performance ratio evaluation for the post-intervention with external prestressed cables.

6 Optimization strategy

In order to perform the optimized strengthening system proposed in this work, a Genetic algorithm was used. Since the above-mentioned optimization problem involves several different issues, a meta-heuristic approach was identified. In particular, the Genetic Algorithm (GA) implemented in Matlab has been adopted due to the low computational effort. Firstly proposed by John Holland in 1975 at the University of Michigan (Holland 1975), and later extended mainly by his student David E. Goldberg (Martí et al. 2018), the algorithm takes inspiration from the natural environment in which individuals with better chance of surviving tends to evolve to the next generation (design vectors related to solutions' attempts with the best fitness in term of Objective Function (OF)) and the core is based directly on the genetic mechanism of transmission of the parents' features to offspring chromosomes adopting specific mathematical operators: crossover operator, mutation operator and selection operator (Plevris 2009). Since its pseudo-random roots, unfortunately, mathematical proofs of its convergence do not exist. However, numerically studies demonstrated that they are able to succeed also dealing with highly non-linear, non-convex and discontinuous domains. Conversely, to mathematical programming hard computing techniques which usually required information about the gradient, GA is considered a soft computing technique because it requires only the OF evaluation with a lower computational effort (Plevris 2009). For this reasons, this paradigm can be ideally transposed to a numerical procedure which leads a population of trial solutions to evolve toward the global optimum of the optimization problem (OF) adapting to the environment which is represented by the feasible region reduced by the presence of the constrains. Substantially, these agents are competing for the resource and only the survival of the fittest to the environment will pass to the next generation (Quaranta et al. 2020). For further readings about the GA and in general to meta-heuristic algorithms, one can refer to e.g. (Martí et al. 2018). Actually, many applications of this optimization strategy can be found in the structural engineering field as for steel, RC and masonry structure (Spillers 2009).

7 Optimization process of the proposed consolidation system

The proposed steel arch strengthening system involves several issues and, in order to propose a reasonable solution from a practical point of view, an optimization process has been performed. Since the arch geometry is fixed because of the chosen typology of PRC beam, it is possible to perform only a size optimization process related to the steel members which compose the trussed arch structure. The main achievement is to optimize the intervention mainly in economic terms in comparison with other more traditional strengthening interventions, e.g. with external prestressed tendons as mentioned in Section 2. Structural optimization can be decomposed in three sub-problems: size optimization, shape optimization and topology optimization (Christensen et al. 2009). In the size optimization process of steel truss structures, the reduction of the steel self-weight, and thus the adopted quantity of steel material, is usually indirectly connected to the reduction of the global cost of the steel structure (Fiore et al. 2016) (Rosso et al. 2021). The objective function (OF) in this case is equal to

$$f_1(\boldsymbol{x}) = W(\boldsymbol{x}) = \sum_{i=1}^{N_{el}} \rho_i V_i(\boldsymbol{x}),\tag{13}$$

in which $\boldsymbol{x}$ is the design vector which defines the parameters referred to the tubular cross section (e.g. external diameter Φ_i and thickness t_i), ρ_i is the steel density ($7, 86$ t/m^3), $V_i(\boldsymbol{x})$ is the volume
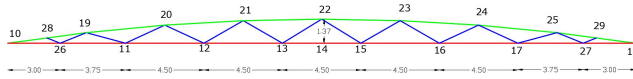
18

Figure 18: Geometry view of the truss model and adopted node numbering (dimensions in meters).

of each steel member and N_{el} is the total number of elements. However, as mentioned in previous Sections, the strengthening system strongly affects the structural behaviour since it is working in parallel with the main structural beam element. Consequently, an effective optimization of the strengthening intervention has to take into account also an OF $f_2(\boldsymbol{x})$ related to the global stiffness K which is directly related to the level of the PRC beam load decrease and the global deformation of the structure δ. As a matter of fact, a trussed arch which satisfies completely $f_1(\boldsymbol{x})$ will result in an excessively slender solution which is useless in terms of structural performances, otherwise, an option which satisfies completely $f_2(\boldsymbol{x})$ will result in an excessive stiff solution which could be an extremely expensive solution.

These two stated aims point towards opposite directions and the best trade-off between the reduction of the steel weight and the increase of the trussed arch stiffness have to be found. Substantially, the optimization problem has to be formally stated as a multi-objective optimization problem. In reality, in (Rao 2019), the simplest approach to solve multi-objective optimization problems is to rewrite the OF to be minimize such as a single-objective optimization problem with a new OF given by a linear combination of the various OFs. In the present case, the single-objective OF becomes as

$$
\begin{aligned}
f(\boldsymbol{x}) &= \alpha \cdot f_{1,\text{adim}} + (1 - \alpha) \cdot f_{2,\text{adim}} \\
&= \alpha \cdot \frac{W(\boldsymbol{x})}{W_{\text{PRC beam}}} + (1 - \alpha) \cdot \frac{|u_{22}|}{u_{\text{beam SW+Q}}}
\end{aligned}
\tag{14}
$$

in which the two OFs have to be non-dimensionalized in order to be able to perform the combination. In particular, the f_1 is divided by the self weight of the PRC beam, $W_{\text{PRC beam}}$, whereas the f_2 is considered as the maximum deformation of the strengthened system monitored at the node 22, as depicted in Figure 18 which is normalized with respect to the mid-span deflection $u_{\text{beam SW+Q}}$ of the non-strengthened PRC beam under the self-weight (SW) and a uniformly distributed live load equal (Q) of 52 kN/m. The α coefficient is a user-defined parameter which allows controlling the relative weight of each OF in the optimization process in a simple and smart way. Since each OF is carrying information related to two opposite objectives, if α is set to 1, the classical single objective size optimization problem is performed but the final solution will be too much slender being useless as a strengthening system. Otherwise, on the other hand, when $\alpha = 0$ the OF will produce the most rigid solutions, very efficient but impracticable and incredibly expensive as a strengthening system. Moreover, in this latter case, the steel truss weight will be too much large also leading to an increase of reactions on piles and abutments. The trussed arch structure is subjected to self-weight and nodal loads due to the connection with the PRC beam which are obtained by the OpenSees model. The OF is constrained because each steel member have to satisfy EN-1993-1-1 safety assessment at Ultimate Limit State in terms of Tensile Force, Compressive Force and Instability verifications as below:

$$
\frac{N_{Ed}}{N_{t,Rd}} \leq 1, \quad \text{where} \quad N_{t,Rd} = \frac{A_i f_y}{\gamma_{M_0}},
\tag{15}
$$

$$
\frac{N_{Ed}}{N_{c,Rd}} \leq 1, \quad \text{where} \quad N_{c,Rd} = \frac{A_i f_y}{\gamma_{M_0}},
\tag{16}
$$

$$
\frac{N_{Ed}}{N_{b,Rd}} \leq 1, \quad \text{where} \quad N_{c,Rd} = \chi \frac{A_i f_y}{\gamma_{M_1}}.
\tag{17}
$$

in which, for the sake of simplicity, class 4 section profiles were excluded. The adopted steel is S355 (f_y = 355 MPa). As depicted in Figure 18, the truss members are parametrized in three categories of tubular section respectively, belonging to the upper arch (green members), diagonal elements (blue members) and lower tie elements (red members). Connecting to OpenSees the Table of properties for steel tubes for circular hollow sections (CHS) which contains 158 different profiles
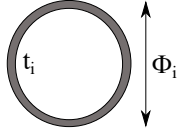
19

Figure 19: Circular hollow cross section (CHS) profiles: a possible parametrization with two design parameters.
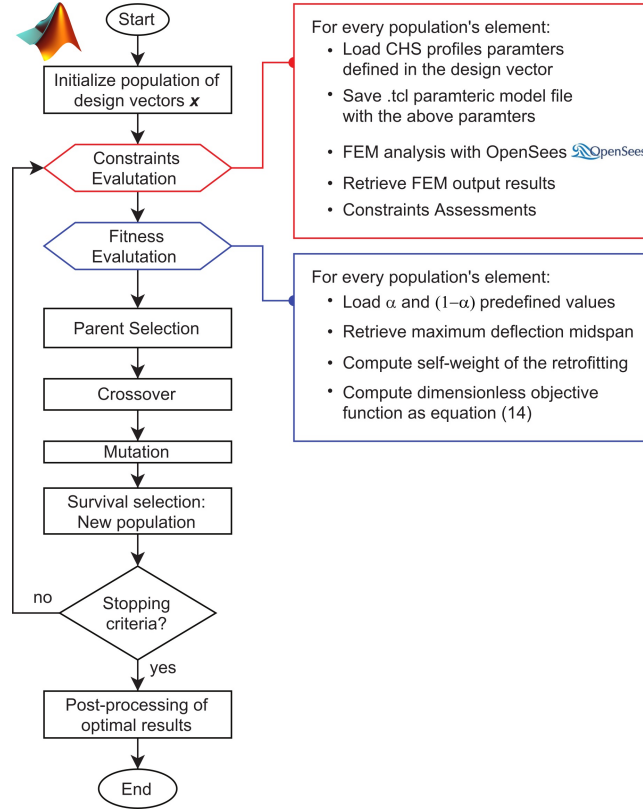

Figure 20: Flowchart of the optimization process using Genetic Algorithm.

(excluding the class 4 section profiles), the design vector is thus completely defined by a vector of three integer numbers $\boldsymbol{x} = [x_1, x_2, x_3]^T$, one for type of truss steel member. Each integer number is referred to a specific row of the Table of properties which identifies all the specifications related to a certain CHS profile located at that row. This strategy produced a less computational cost with respect to optimize the two design variables (Φ_i, t_i) as depicted in Figure 19 for each element type as continuous variables. For the current study, a population size of 100 individuals was chosen with a stopping criterion referred to the achievement of a maximum number of prescribed iterations set to 100. The flowchart in Figure 20 describes, from a conceptual point of view, how the optimization was performed in Matlab environment and how the constrains have been managed.

8   Results and Discussion

Solving the optimization problem presented in the previous Section, during each iteration of GA, a population of solutions' attempts is considered and, for each individual, Matlab will compile a OpenSees file to build the model with the characteristics defined by each individual. Thereafter, Matlab launches OpenSees analysis and finally it retrieves the FEM results in order to perform the final constraints verification and evaluate the fitness of each individual. Firstly, the two limit cases were analyzed with $\alpha = 1$ and $\alpha = 0$. As reported in Table 14, it is evident that none of the
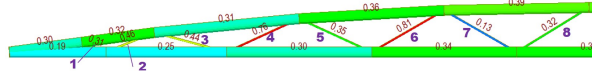
Figure 21: Geometric lateral view of the optimal trussed arch system with annotations regarding to the performance ratio of each steel member.
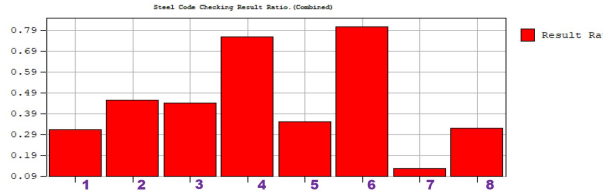

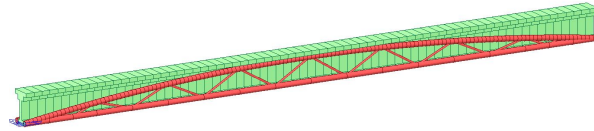Figure 22: Performance ratios of steel diagonals members obtained with MidasGen$^{\copyright}$ software.

Figure 23: Three-dimensional view of MidasGen$^{\copyright}$ model of the optimal found solution.

two limit case can be considered as an optimal trade-off between the two opposite OFs aims. As a matter of fact, with $\alpha = 1$ the trussed arch structure seems to be useless in terms of load reduction of the PRC beam; instead, on the opposite, with $\alpha = 0$ the self weight of the steel trussed arch is too much heavy. In the present study, it was found that values of α comprised between $0,6$ and $0,7$ allow solutions technically practicable, respectful of all the constraints verifications, with an optimal balance between material consumption and the global stiffness of the strengthened beam. A value of $\alpha > 0,5$ means that a greater weight is associated to the size optimization OF, but always taking into account also a not negligible influence of the OF related to the global stiffness of the system. In Table 15, solutions obtained for $\alpha = 0,6$ and $\alpha = 0,7$ are illustrated where the structural efficiency is reported in terms of performance coefficient given by the ratio between the acting moment and resisting moment M_{Sd}/M_{Rd} after the strengthening intervention, always referred to the four degradation levels considered in the current study.

Results in Table 15 show promising strengthening solutions effectively able to deal with degradation levels 1, 2 and 3. Furthermore, the obtained CHS profiles are reasonable to perform this kind of intervention. Since with $\alpha = 0.6$ the OF is greater weighted towards maximization of global stiffness with respect to the minimization of the steel SW, it is reflected by the consistent increase of the total steel SW which almost redoubled with respect to the case $\alpha = 0.7$. Through the adoption of the tool design in MidasGen$^{\copyright}$ software, the final results were assessed to be respectful of the stress and buckling constraints and the performance ratio of each element has been depicted in Figures 21 and 22. A three-dimensional view of MidasGen$^{\copyright}$ model of the optimal found solution is illustrated in Figure 23. As shown in these figures, there is apparently a non-optimal distribution of the performance ratios. In reality, it is necessary to recall that calibrating the α coefficient, it allows to optimize not only the minimization of the steel SW but also considering to reach a reasonable global stiffness to produce an actual effective strengthening system. In order to further push the optimization process in terms of performance ratio for each steel member, it would be virtually possible to also parametrize the diagonal elements with two different CHS profiles when they are in prevalent compression or tension under the current load configuration without compromise the overall global stiffness.

Effects of α coefficient

α	$1-\alpha$	PRC beam load decrease [%]	SW steel trussed arch [t]
0	1	0,1%	0,3
1	0	78%	58

Table 14: Effects of α coefficient

Results of optimal strengthened PRC beams.

α	CHS Arch [mm]	CHS Lower tie [mm]	CHS Diagonals [mm]	Steel SW [t]	Degradation level	$\frac{M_{Sd}}{M_{Rd}}$
0.7	$\phi 323,9$ $t.\,6$	$\phi 323,9$ $t.\,6$	$\phi 60,3$ $t.\,2,5$	3,54	1 2 3 4	0,89 0,93 0,98 1,03
0.6	$\phi 323,9$ $t.\,12$	$\phi 323.9$ $t.\,12$	$\phi 114,3$ $t.\,3$	6,95	1 2 3 4	0,82 0,86 0,90 0,95

Table 15: Results of optimal strengthened PRC beams for $\alpha = 0,6$ and $\alpha = 0,7$.

9 Preliminary cost comparison with traditional strengthening interventions

In order to the proposed strengthening system evaluate also from an economic point of view , a preliminary comparison with the traditional external prestressing cables technique is performed. It is necessary to underline the preliminary level of this kind of evaluation, since some other technological aspects have to be fully investigated in the future, e.g. the connections design of the trussed arch element to the PRC beam. Furthermore, labour cost, technological aspects, etc. are considered in a very simplified manner taking into account unitary cost coming from some quoted works and Italian documents related to external tendons strengthening intervention and steel unitary cost. In a more refined economic analysis all of the previous aspects have to be deeper analysed.

In (ANAS 2021), the steel unitary cost for truss beams with span length range 25-45 m can be considered as 2,59 €/kg which comprises materials cost and also launching operations. Instead, in (Devitofranceschi 2018), in a simplified manner, four external prestressing cables can be considered an all-encompassing unitary cost (launching, anchorages, pretensioning operations) as 526 €/m for the intervention with two cables with 7 strands each, or 878 €/m for a solution with four external cables. In this case, two different solutions are considered in order to obtain a range of variability for the cost of external cable interventions in comparison with the two optimal trussed arch solutions obtained with $\alpha = 0,6$ or $0,7$. Based on the previous data, the overall global preliminary costs are reported in Table 16. Based on that preliminary estimations, it is possible to state that the steel trussed arch with $\alpha = 0,7$ is the most economic intervention because it is slightly lower than the external tendon solution with two cables. It is worth noting that, even considering different levels of degradation, the unitary cost for external prestressed cables solution does not change because, for different degradation levels, only the prestressing forces of the tendons vary and its unitary cost is mainly related to technological issues such as the design of anchorages, positioning hydraulic jacks, etc. On the other hand, the proposed trussed arch strengthening solution could virtually require cheaper truss structures, more optimized, lighter and slender for lower levels of degradation. Instead, as shown in the previous Section, for higher levels of degradation, it is not reasonable to overcome $\alpha = 0,7$ because it may result in a structure excessively light and slender thus the percentage of PRC beam load decrease could be virtually almost negligible. Eventually, comparing the costs in Table 16 for $\alpha = 0,7$ and for a four tendons solution, these values appear to be higher than the two other solutions but they are always comparable at this preliminary stage, underlining once again the engineering relevance of the optimal found solution.

	Unitary cost	Quantity	Cost
Preliminary economic comparison among consolidation interventions.			
Trussed arch $\alpha = 0.6$	2,59 €/kg	$2 \cdot 6.95 = 13,9$ t	36'000 €
Trussed arch $\alpha = 0.7$	2,59 €/kg	$2 \cdot 3.54 = 7,08$ t	18'337 €
Ext. prestr. with 2 cables	526 €/m	36 m	18'936 €
Ext. prestr. with 4 cables	878 €/m	36 m	31'608 €

Table 16: Preliminary economic comparison among traditional consolidation interventions with two or four external prestressed cables with the proposed optimal trussed arch strengthening system with $\alpha = 0,6$ and $\alpha = 0,7$.

10 Some remarks about resilience

Referring to the study conducted by (Cimellaro et al. 2010), the concepts of disaster resilience and its evaluation are taken into account. In this section, a discussion about the resilience of the proposed strengthening system is proposed using a common framework. Researchers at the Multidisciplinary Center for Earthquake Engineering Research (MCEER), have identified four dimensions along which resilience can be improved. These are *robustness, resourcefulness, redudancy and rapidity.*

Rapidity is the "*Capacity to meet priorities and achieve goals in a timely manner in order to contain losses and avoid future disruption*". In our case study, *Rapidity* consists of the efficiency and restoration time of the intervention. As shown in section 9, the advantage to choose the proposed retrofitting system to the traditional one is not only economical but also in terms of required installation time. Each element composing the strengthening system can be realized entirely in the factory, afterwards assembled in-situ and finally connected to the damaged structure without such complex procedures or equipment. In this way, any waste of time would be avoided.

Robustness is, referring to engineering systems, "*the ability of elements, systems or other units of analysis to withstand a given level of stress, or demand without suffering degradation or loss function*". The concept of the proposed system allows a reasonable robustness level of the consolidated structure. Therefore, if a given level of stress threats the structural health or contributes to the capacity reduction of the concrete beam, the reinforcing system will provide its beneficial effect.

The concept of *redundancy*, defined as "*the quality of having alternative paths in the structure by which external forces can be transferred, which allows the structure to remain stable and safety following the failure of any single element*", it is strictly correlated to the *robustness* of a structure. By coupling an arch resisting system to the damaged beam means increasing the high of *redundancy* of the whole system. The geometry of the retrofitting system was designed in order to allow some local failure, for example at the level of trusses, without compromising the functionality of the structure. In this way, alternative load paths are introduced and the safety of the consolidated beam is guaranteed. Furthermore, the presence of several connections at different levels between the steel arches and the consolidated prestressed beam provides an additional positive contribution to *redundancy* of the beam-arches system.

Finally, the concept of *resourcefulness* is taken into account, defined as "*the capacity to identify problems, establish priorities, and mobilize resources when conditions exist that threaten to disrupt some element, system, or other unit of analysis*". Therefore, this is a property difficult to quantify since it mainly depends on human skills and preparedness during extreme events or emergencies, the proposed system could contribute positively. When damage occurs into any element of a bridge, any traditional intervention method provides a solution that limits or, in extreme cases, blocks the operativity of the structure disrupting traffic and vehicle movement. The proposed retrofitting system in this work could present the advantage of being realized to ensure, at least partially, the functionality of the transport network during the retrofitting intervention and further future studies may address this important issue for network transport resilience evaluation.

11 Conclusion

In this work, a new strengthening system, as an alternative to the traditional external prestressing cables method, has been proposed along with an efficiency index. This last includes both the economic impact and the structural performance.

A parametric modeling has been performed in order to investigate the variables that mainly affect the industrial solution considered as the target of this work. The double-pinned supports static scheme appears to be the stiffest solution despite several configurations investigated. The geometric and material features of the circular hollow sections (CHS) for each structural element, composing the proposed strengthening system, exhibit the greatest gyroscopic inertia in comparison with other cross section typologies with the same area. In this way, a maximum centrifugal mass effect is achieved in order to increase the efficiency of the strengthening system. Moreover, the sensitivity analysis shows how the proposed solution is strongly dependent on the dimensional characteristics of the compression and tension chords rather than truss diagonal elements: increasing the size of the arch and tie elements, a significant improvement in the efficiency of the system is recognized due to their main contribution to the centrifugal mass effect. For these reasons, structural optimization was performed in order to prefer this kind of structural characteristics. The optimization process allows to detect the best solution as the best trade-off in terms of stiffness and self-weight of the proposed solution. The multi-objective optimization problem has been reconducted to a single objective problem through an OF weight parameter α and its complementary $(1 - \alpha)$ for the two counterposed OFs. The parameter α has been evaluated with the aim to identify the equilibrium solution which guarantees the lighter strengthening system with the highest stiffness. In conclusion, the optimization model allows capturing, when 20% of the area loss occurs (degrade level 3), until to 40% of the total external distributed load. Finally, an economic estimation of the consolidation system installation has been presented comparing the total cost of the proposed retrofitting technique with the traditional external prestressing one. Although a significant cost saving is not found, it is worth noting that the proposed procedure allows the production of the beam-arch assemblage entirely on site without the need of skilled workers or specialist companies. Moreover, the proposed retrofitting technique does not need an estimation of the residual prestressing level, which could increase the compression stress configuration of the concrete beam without any beneficial effects. As future developments, it will be interesting to conduct a detailed design of the connection between the concrete beam and the strengthening system and provide a topological optimization with the aim to verify the optimal shape of the consolidation system. Furthermore, a complete analysis that will take into account realistic bridge actions (not only the vertical one but also horizontal components of wind and earthquake, for example) on the beam with the modeling of the entire deck considering the global behavior of the structure, will be the further development of the research.

References

Kashani MM, Maddocks J and Dizaj EA (2019) Residual capacity of corroded reinforced concrete bridge components: State-of-the-art review. *Journal of Bridge Engineering ASCE*, **24(7)**:03119001.

Di Ludovico M, Prota A, Manfredi G and Cosenza E (2010) FRP strengthening of full-scale PC girders. *Journal of Composites for Construction ASCE*, **14(5)**:510–520.

Petrangeli MP, Fieno L and Orlandi R (2019) Valutazione della sicurezza in esercizio dei ponti esistenti con impalcati in c.a.p. *INGENIO* (https://irp-cdn.multiscreensite.com/82d19c8d/files/uploaded/sicurezza-ponti-esistenti-impalcati-cap-petrangeli.pdf).

Petrangeli MP (2017) Progettazione e costruzione di ponti con cenni di patologia e diagnostica delle opere esistenti. *Casa Editrice Ambrosiana*.

Bazzucchi F, Restuccia L and Ferro GA (2018) Considerations over the Italian road bridge infrastructure safety after the Polcevera viaduct collapse: past errors and future perspectives. *Frattura e Integrita Strutturale*, **12**.

Domaneschi M, Pellecchia C, De Iuliis E, Cimellaro GP, Morgese M, Khalil AA and Ansari F (2020) Collapse analysis of the Polcevera viaduct by the applied element method. *Engineering Structures*, **214**:110659.

Morgese M, Ansari F, Domaneschi M and Cimellaro GP (2020) Post-collapse analysis of Morandi's Polcevera viaduct in Genoa Italy. *Journal of Civil Structural Health Monitoring*, **10(1)**:69–85.

Park YH, Park C, Park YGul (2005) The behavior of an in-service plate girder bridge strengthened with external prestressing tendons. *Engineering structures*, **27(3)**:379–386.

Arici M and Granata MF (2019) Prevenzione del degrado dei ponti in cap con la precompressione bilanciata. Il ponte funicolare. *Seminario Internazionale CIAS*.

Godart B (2015) The behavior of an in-service plate girder bridge strengthened with external prestressing tendons. *Structure and Infrastructure Engineering*, **11(4)**:501–518.

Recupero A, Spinella N and Tondolo F (2018) A model for the analysis of ultimate capacity of RC and PC corroded beams. *Advances in Civil Engineering*, **2018**.

Daly AF and Witarnawan W (1997) Strengthening of bridges using external post-tensioning. *Conference of eastern Asia society for transportation studies*, Seoul, Korea.

Highways agency (1999) Post-tensioned concrete bridges: Anglo-French liaison report. *Service d'etudes techniques des routes et autoroutes*, Telford.

Pisani MA (1999) Strengthening by means of external prestressing. *Journal of Bridge Engineering ASCE*, **4(2)**:131–135.

Alqam M and Alkhairi F (2019) Numerical and analytical behavior of beams prestressed with unbonded internal or external steel tendons: a state-of-the-art review. *Arabian Journal for Science and Engineering*, **44(10)**:8149–8170.

Khudeira S (2010) Strengthening of deteriorated concrete bridge girders using an external posttensioning system. *Practice Periodical on Structural Design and Construction*, **15(4)**:242–247.

Franciosi V (1971) archi. *Scienza delle costruzioni*, **3(2)**:208–209.

Fiore A, Marano G C, Greco R et al. "*Structural optimization of hollow-section steel trusses by differential evolution algorithm*". Int J Steel Struct 16, 411–423 (2016).

Rao Singiresu S, *Engineering Optimization Theory and Practice*, John Wiley & Sons, Fifth Edition, USA (2019)

Plevris V *Innovative Computational Techniques for the Optimum Structural Design Considering Uncertainties*, National Technical University of Athens, Athens (2009)

Martí R, Pardalos P M, Resende M G "*Handbook of Heuristics*", Springer Nature Switzerland (2018)

Holland J H (1975) "*Adaptation in Natural and Artificial Systems*", University of Michigan Press, Ann Arbor, Michigan.

ANAS - Gruppo FS Italiane, "*Elenco prezzi 2021 - Nuove Costruzioni e Manutenzione Straordinaria*", Direzione Ingegneria e Verifiche, (2021).

Devitofranceschi A., (2018) "*Riparazione di viadotti stradali in precompresso: tecniche di intervento ed analisi costi benefici*", in Italian Concrete Days - AICAP, Lecco.

Gaßner G. and Kollegger J (2021), "*Integrale Bogenbrücke mit Zugband.* Beton- und Stahlbetonbau, 116: 127-138.

Clemente P (2020) "*Monitoring and evaluation of bridges: lessons from the Polcevera Viaduct collapse in Italy*". Journal of Civil Structural Health Monitoring 10, 177–182.

Zhao G, Xu J, Li Y and Zhang M (2018) *"Numerical Analysis of the Degradation Characteristics of Bearing Capacity of a Corroded Reinforced Concrete Beam"*, Hindawi, Advances in Civil Engineering, vol. 2018, Article ID 2492350, 10 pages.

Rosso M M, Cucuzza R, Di Trapani F and Marano G C (2021) *"Nonpenalty Machine Learning Constraint Handling Using PSO-SVM for Structural Optimization"*, Hindawi, Advances in Civil Engineering, vol. 2021, 17 pages.

Cucuzza R, Rosso M M and Marano G C (2021) *"Optimal preliminary design of variable section beams criterion"*, Springer Nature journal, Springer Nature Applied Sciences, vol. 2021,12 pages.

Christensen P W et al. (2009) *"An Introduction to Structural Optimization"*, Springer Netherlands, Springer Science+Business Media B.V. .

Quaranta G & Lacarbonara W (2020) *"A review on computational intelligence for identification of nonlinear dynamic systems"*, Nonlinear Dyn 99, 1709-1761.

Spillers W. R (2009) *"Structural Optimization"*, pp. 1-5, Springer-Verlag, US, Berlin, Germany.

Cimellaro G. P, Andrei M. Reinhorn & Michel Bruneau (2010) *"Framework for nalytical quantification of disaster resilience"*, ELSEVIER, Engineering Structures.